Received: 8 October 2018 | Revised: 21 January 2019 | Accepted: 25 February 2019

DOI: 10.1002/htj.21449

WILEY

RESEARCH ARTICLE

Numerical validation of natural convection heat transfer with horizontal rectangular fin array using straight knurling patterns on fins—correlation for Nusselt number

Rahul C. Chikurde[1] | **Basavraj S. Kothavale Dr. Prof.**[1] | **Narayan. K. Sane Dr.**[2]

[1]Department of Mechanical Engineering, MIT COE, Affiliated to SSPU, Pune, India

[2]Emeritus Professor, Walchand College of Engineering, Sangli, India

Correspondence
Rahul C. Chikurde, Department of Mechanical Engineering, MIT COE, Kothrud 411038, Pune, Affiliated to SSPU, Pune, India.
Email: rcchikurde@gmail.com

Abstract

Natural convection heat transfer from horizontal rectangular fin array with various knurling patterns has been studied experimentally by the present authors to investigate the effect of knurl-produced surface roughness of fin on the heat transfer rate. The parameters like knurling height from base, knurling depth, fin spacing, and supply wattage were considered for parametric study. In the present paper, numerical method (CFD) is used to simulate natural convection phenomena with knurled fins and results are validated with the experimental data available from literature. The numerical results show similar trends compared with experimental data and one can use this method to study various fin configurations for knurling patterns. The flow patterns from experiments and numerical method are compared for different supply wattages and fin spacing to back up the conclusion. It is also observed that the variation in nondimensional roughness depth and spacing (D_{kn}/H and S/H) have more effect on Nusselt number than roughness height parameter (H_{kn}/H). Further, the method is extended to study numerically large number of fin configurations with knurling patterns to gather sufficient data for Nusselt number with respect to fin

geometric parameters as above and establish correlation for heat transfer coefficient for such type of fins.

KEYWORDS
fin spacing, horizontal rectangular fin array, knurling depth, knurling height, knurling patterns, natural convection heat transfer, numerical method (CFD), turbulence

1 | INTRODUCTION

Cooling of electronic devices has gained attention of many researchers in view of increasing power dissipation and hence requirement for efficient cooling so as to maintain acceptable temperatures. There is need to employ modern techniques of heat transfer augmentation or combination of such techniques so as to keep the electronic devices cool throughout the operating life. Researchers have studied many passive heat transfer augmentation techniques such as

1. Fins with varying contact ratio with base plate
2. Perforated fins—triangular, circular, square, hexagon, and rectangular
3. Convergent-divergent fins
4. V-type fin-arrays
5. Fins with dimples
6. Plate fin-pin fin combination
7. Surfaces using protrusions (ribbed, stepped, and wavy)

Most of the above work is carried out on vertical, inclined base plate arrays, triangular channels, and so forth. In the present paper, unique approach of knurled fins to augment the heat transfer is studied numerically and the results are validated with available literature data and also from experiments. An attempt is made to develop correlation for Nusselt number in terms of Rayleigh number and nondimensional fin roughness parameters.

2 | GOVERNING EQUATIONS OF FLUID FLOW APPLICABLE TO NATURAL CONVECTION HEAT TRANSFER

The natural convection flow is modeled by a set of elliptic partial differential equations describing the conservation of mass, momentum, and energy in three rectangular cartesian coordinate directions. As in forced convection, inertia, and viscous effects, energy transfer by advection and diffusion remain important in free convection. The difference lies in major role played by buoyancy forces, which help to sustain the flow in free convection.

$$\frac{\partial(\rho u)}{\partial x} + \frac{\partial(\rho v)}{\partial y} + \frac{\partial(\rho w)}{\partial z} = 0, \tag{1}$$

$$\frac{\partial(\rho u^2)}{\partial x} + \frac{\partial(\rho uv)}{\partial y} + \frac{\partial(\rho uw)}{\partial z} = -\frac{\partial P}{\partial x} + \rho\vartheta\left(\frac{\partial^2 u}{\partial x^2} + \frac{\partial^2 u}{\partial y^2} + \frac{\partial^2 u}{\partial z^2}\right), \tag{2}$$

$$\frac{\partial(\rho vu)}{\partial x} + \frac{\partial(\rho v^2)}{\partial y} + \frac{\partial(\rho vw)}{\partial z} = -\frac{\partial P}{\partial y} + \rho\vartheta\left(\frac{\partial^2 v}{\partial x^2} + \frac{\partial^2 v}{\partial y^2} + \frac{\partial^2 v}{\partial z^2}\right) + g(\rho - \rho_a), \tag{3}$$

$$\frac{\partial(\rho wu)}{\partial x} + \frac{\partial(\rho wv)}{\partial y} + \frac{\partial(\rho w^2)}{\partial z} = -\frac{\partial P}{\partial z} + \rho\vartheta\left(\frac{\partial^2 w}{\partial x^2} + \frac{\partial^2 w}{\partial y^2} + \frac{\partial^2 w}{\partial z^2}\right), \tag{4}$$

$$\frac{\partial(\rho uT)}{\partial x} + \frac{\partial(\rho vT)}{\partial y} + \frac{\partial(\rho wT)}{\partial z} = \frac{\vartheta}{Pr}\left(\frac{\partial^2 T}{\partial x^2} + \frac{\partial^2 T}{\partial y^2} + \frac{\partial^2 T}{\partial z^2}\right). \tag{5}$$

In Equation (3) above, the quantity $(\rho - \rho_a)$ can be calculated using Boussinesq approximation, which is $(\rho - \rho_a) = \rho\beta(T_\infty - T)$. Gray and Giorgini showed that the error due to the Boussinesq approximation is less than 10% for air as long as $\Delta T \leq 28.6°C$. However, in the present simulations, the temperature differences are up to 90°C, hence the Boussinesq approximation was not used. The assumptions used in the governing equations are in agreement with steady, incompressible, laminar flow of air with constant properties, except for density which is taken as a function of temperature only. The change in the Pr number with temperature was found to be negligible and a constant value of $Pr = 0.70$ was used.

2.1 | Nondimensional numbers in Natural Convection

Grashof number plays the same role in free convection that the Reynolds number plays in forced convection. It indicates the ratio of buoyancy force to the viscous force acting on the fluid.

$$Gr_L = \frac{g\beta(T_s - T_\infty)L^3}{\upsilon^2}, \tag{6}$$

where L is characteristic dimension and υ is kinematic viscosity of fluid (μ/ρ).

Transition in a free convection boundary layer depends on the relative magnitude of the buoyancy and viscous forces in the fluid. Rayleigh number, which correlates the occurrence of turbulence is defined as the product of Grashof and Prandtl numbers $(Ra = Gr \cdot Pr)$.

$$Ra_L = \frac{g\beta(T_s - T_\infty)L^3}{\alpha\upsilon}. \tag{7}$$

The transition to turbulence has a strong effect on the heat transfer. The correlations developed for laminar flow apply if $Ra \leq 10^9$.

3 | REVIEW OF LITERATURE

Baskaya et al[1] carried out systematic investigation of the effects of fin spacing, fin height, fin length, and temperature difference between fin and surroundings on heat transfer from horizontal fin arrays. They used numerical technique to simulate several cases reported in the literature. After obtaining a good agreement with results from the literature, a large number of runs were performed for a detailed parametric study. It was found that interactions among all the design parameters must be considered. The results are presented in graphical form together with optimum values along with correlations, and compared with available experimental data from the literature. The overall heat transfer is enhanced with increase in fin height and decrease in length of the fin. In addition, for maximum heat transfer the optimum values of fin spacing were obtained. Bhavnani et al[2] used interferometric technique to determine local heat transfer coefficients (HTCs) for rough surfaces with steps and ribs. They studied influencing parameters, such as inclination angle and height to spacing ratio, and found that 23.2% increase of HTC with step pitch to height ratio of 16. However ribbed surfaces resulted in performance degradation compared with plane fin. Kwak et al[3] studied natural convection heat transfer from vertical surfaces having longitudinal grooves. They observed secondary recirculation flows in the grooves that obstruct the main flow into the groove and thus results in lowering the heat transfer. It is found that the Nusselt number is maximum at the outer surface of the protrusion. They proposed correlation for Nu in terms of Ra using the numerical technique. Jiang et al[4] studied convection heat transfer in a rectangular channel with inclined ribs on one wall using experiments and numerical analysis. Comparisons between the experimental and numerical results showed that the SST k-ω turbulence model was more suitable for the convection heat transfer in such channels than the RNG k-ε turbulence model. The numerical results showed that the HTCs were largest with the 60° ribs, but the channel with the 20° ribs gives the best overall thermal performance with 4 mm spacing between ribs. Chaube et al[5] conducted computational analysis of heat transfer augmentation and flow characteristics due to roughness in the form of ribs on a broad, heated wall of a rectangular duct for turbulent flow with Reynolds number ranging from 3000 to 20 000. Shear stress transport k-ω turbulence model is used by comparing the predictions of different turbulence models with experimental results available in the literature. The analysis shows that peak in local HTC occurs at the point of reattachment of the separated flow. The results predict significant enhancement of heat transfer due to roughness in comparison with that of a smooth surface. There is a good matching between the predictions by SST k-ω model and experimental results. Layek et al[6] investigated heat and fluid flow characteristics of fully developed turbulent flow in a rectangular duct having repeated integral transverse chamfered rib-groove roughness. Reynolds number ranging from 3000 to 21 000, relative roughness pitch of 4.5 to 10, chamfer angle of 5° to 30°, relative groove position of 0.3 to 0.6, and relative roughness height of 0.022 to 0.04. The effect of roughness parameters on Nusselt number and friction factor have been discussed and found that the maximum heat transfer enhancement occurs for the relative roughness pitch of six and relative groove position of 0.4. Further the friction factor increase monotonously with an increase in chamfer angle. Correlations have been found for Nusselt number and friction factor with average absolute percentage deviation of 2.8% and 2.4%, respectively, in the range of parameters investigated. Ashjaee et al[7] studied flow along an isothermal vertical wavy surface experimentally and

numerically. Parameters like amplitude-wavelength ratio "a" and the Rayleigh number were considered. From their study, authors observed that the average HTC decreased as the amplitude-wavelength ratio increased and the reduction of the average HTC for the wavy surface with $a = 0.2$ was significant. The total convective heat transfer rate increased as the amplitude-wavelength ratio increased. This was due to the increase in the heat transfer area. Finally, the experimental data were correlated with a single equation which gave the local Nusselt number along the surface as a function of the amplitude-wavelength ratio and the Rayleigh number. Shaeri et al[8] carried out three-dimensional numerical study of turbulent fluid flow and convective heat transfer over an array of solid and perforated fins. Perforations such as small channels in several numbers are arranged along the length of fins. Effects of flow and perforations on heat transfer rate are determined and comparison between solid and perforated fins is accomplished. Reynolds numbers varied from 2e04 to 4e04. Average friction drag for perforated fins is higher compared with the solid fin due to higher contact area. The recirculation zone around the lateral surfaces of fin reduced and fin effectiveness increased with an increase in number of perforations. A similar study as above has been conducted by Ismail et al[9] numerically by using RNG-based k-ε turbulence model to study turbulence flow parameters for perforated fins arrays. Fins with circular perforations showed remarkable heat transfer enhancement and reduced pressure drop. The results of this study also helped in designing microheat sinks for heat removal from electronic devices. Ismail et al[10] have used modified k-ω turbulence model to evaluate flow and heat transfer parameters on fins with lateral perforations of square, circular, triangular, and hexagonal cross-sections. They found that triangular perforated fins have the lowest and solid fins have the highest Nusselt number values. Further hexagonal shape gives highest fin effectiveness. Shadlaghani et al[11] studied numerically triangular fins with and without longitudinal perforations. They showed that increased height/thickness ratio enhanced the heat transfer rate. Square and circular cross section perforations gives almost equal enhanced performance compared with triangular fin. Raut et al[12] studied knurled fin arrays experimentally and found that knurling height, depth, and fin spacing affect the HTC and they found 10% to 15% augmentation with specific knurled fin array configuration. Chikurde et al[13] reviewed various augmentation techniques for fins with perforations, protrusions and classified previous studies in terms of different fin types, longitudinal or lateral perforations, and various surface roughness elements used to enhance heat transfer. They listed major finding and conclusions from these studies and also mentioned future scope of study with knurling and slit patterns as form of surface roughness on fins.

4 | DETAILS OF NUMERICAL MODEL SETUP

4.1 | Fin geometry and surrounding domain

Symmetric nature of plane fin along with surrounding domain allows for reduction of actual computational domain to one-half or one-fourth of full model size. Numerical model of fin is built using a CFD preprocessor. Meshing and all boundary conditions are generated and imported in commercial CFD software and problem set-up is done. Natural convection is enabled by including effect of gravity. Side and center symmetry is used to reduce the model size. The fin is assumed to be at constant temperature T_s, that is, isothermal fin. The base of the fin is also kept at same temperature. Ambient is kept at

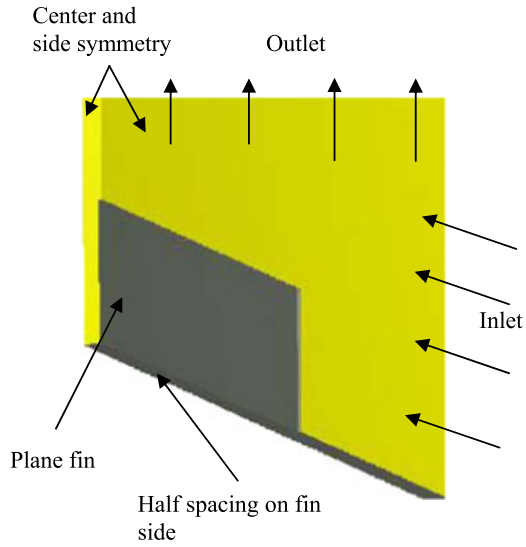

FIGURE 1 Numerical model of plane fin geometry and surroundings [Color figure can be viewed at wileyonlinelibrary.com]

300 K (T_a) so that the temperature difference between fin surface and ambient becomes ($T_s - T_a$). Zero pressure inlet and pressure outlet boundary conditions are used at domain inlet and outlet, respectively. Generally, the mesh size of the model is kept between 0.5 and 1 Mn depending on fin configuration and spacing. This gives sufficiently accurate results.

4.2 | Choice of turbulence model

For plane fin configuration, laminar flow model is considered and for fins with knurling patterns, two equation SST K-ω low Reynolds number model is used to capture flow instabilities due to knurling. Few constants of this turbulence model are optimized so as to validate with experimental results. The mesh near fin walls is kept such that y^+ requirement of K-ω turbulence model (~1-10) is met with converged solution.

4.3 | Discretization schemes and convergence criteria

Numerical solution is started with first order accuracy for momentum, pressure, and energy and other turbulent scalar equations. With this, scaled residuals are allowed to fall below 1e-3 for about 500 iterations. After that, body force weighted discretization for pressure and second-order upwind scheme for momentum equation are used. For about another 500 iterations, the scaled residuals are allowed to fall below 1e-4. During the solution, convergence history for HTC on fin surfaces is observed. The convergence is obtained when the value of HTC does not change in subsequent iterations. Figures 1 and 2 show computational domain with plane and knurled fin, respectively, with inlet and outlet boundary conditions.

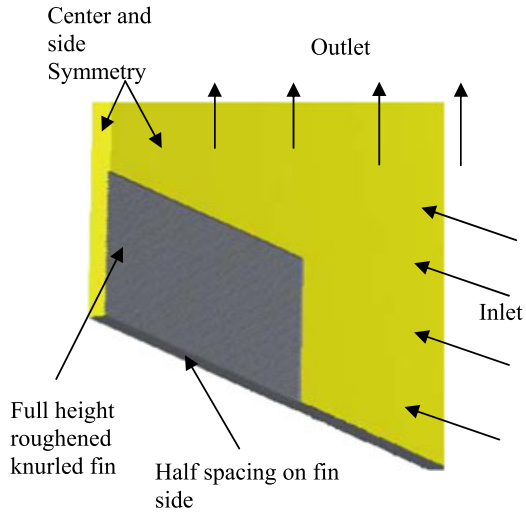

FIGURE 2 Numerical model of knurled fin geometry and surroundings [Color figure can be viewed at wileyonlinelibrary.com]

5 | GRID INDEPENDENCY STUDY

The geometry of fin and surroundings, that is, computational domain is generated in commercial preprocessing package and the mesh is generated using various schemes. Care is taken so that all cells are hexahedral since the plane fin geometry allows high quality hex mesh to be generated. One can have close control on the mesh size or cell count using edge/surface mesh controls and grading. It is seen that near-wall quantities vary as the cell count varies. Thus with increasing number of cells, the variation in these quantities become negligible and the values remain constant for further increase in cell count. This calls for grid independency study to be carried out for the problem under consideration so that optimum value of cell count can be determined.

Figure 3 shows variation of Nusselt Number (*Nu*) with respect to cell count. It is seen that value of *Nu* is higher with coarse meshes and reduces with increase in cell count. After around 0.7 Mn cell count, the variation in *Nu* value becomes negligible and increasing cell count beyond 1 to 1.2 Mn does not yield better accuracy. Hence, it was decided to use cell count in the range of 0.5 to 1 Mn depending on fin configuration so as to get good accuracy with lesser computational time.

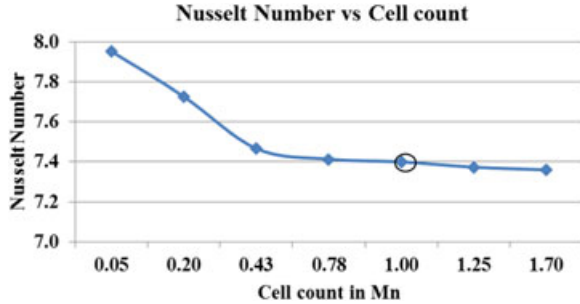

FIGURE 3 Nusselt number variation vs cell count in Mn [Color figure can be viewed at wileyonlinelibrary.com]

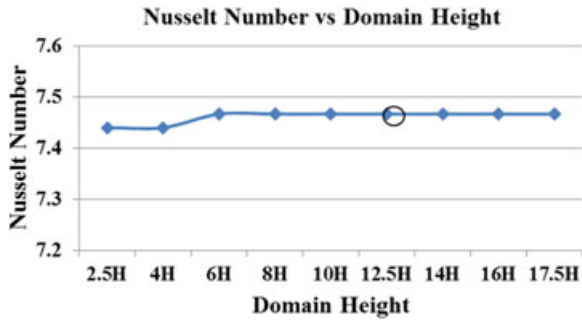

FIGURE 4 Nusselt number variation vs domain height [Color figure can be viewed at wileyonlinelibrary.com]

TABLE 1 Cell count vs Nusselt number

No. of cell counts with adaption around fin (Mn)	Nusselt number	No. of cells in boundary layer
0.43	7.68	3
0.82	7.52	6
1.27	7.50	8
1.55	7.45	10

Also as the domain height is increased beyond 10H, the Nusselt number becomes constant and further increase in height does not affect its value. Thus, in all numerical analysis, appropriate domain height is taken as 12.5H as shown in Figure 4 below.

Further to this, another study was carried out by increasing number of cells near the fin in the boundary layer using grid adaptation technique. Table 1 shows the result of the numerical simulation with adaptation around fin. It is seen from Figure 5 that cell count around 0.8 to 1 Mn may be used so as to get good accuracy.

6 | NUMERICAL MODEL VALIDATION WITH RESULTS FROM LITERATURE

Harhap and McManus[14] have presented experimental results for various flat fin horizontal array sets with different conditions. The HTC was plotted against excess temperature

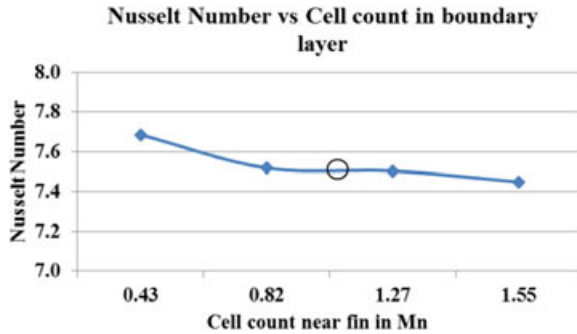

FIGURE 5 Variation of Nusselt number with cell count around fin [Color figure can be viewed at wileyonlinelibrary.com]

TABLE 2 Cases for numerical simulation

Case #	Set no.	2*L*, mm	*H*, mm	*S*, mm	th, mm
Case 1	IV-2L10	254	25	8.0	1.0
Case 3	III-2L5	127	38	6.4	1.3

Abbreviations: H, fin height; *L*, half fin length; *S*, spacing between two fins; th, fin thickness.

difference and they propose generalized correlation in terms of nondimensional group of parameters.

For the two cases from above reference, numerical model is developed and with same temperature difference, the model is validated by predicting HTC so as to compare with the experimental data. Cases considered are as shown in Table 2.

Below plots in Figures 6 and 7 show the comparison of available experimental data and numerical results.

It can be seen that, for cases 1 and 3, there is very good agreement (~10%) between experiment and numerical results. Thus, the numerical model is validated and can be used further for simulation with different fin configurations.

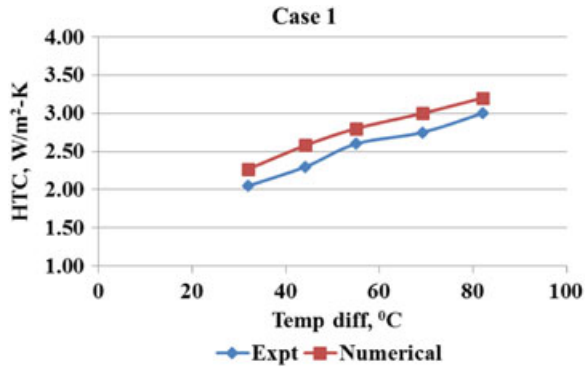

FIGURE 6 Heat transfer coefficient vs temperature difference for case 1 [Color figure can be viewed at wileyonlinelibrary.com]

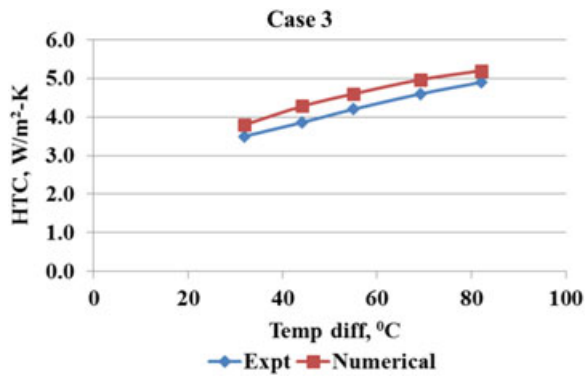

FIGURE 7 Heat transfer coefficient vs temperature difference for case 3 [Color figure can be viewed at wileyonlinelibrary.com]

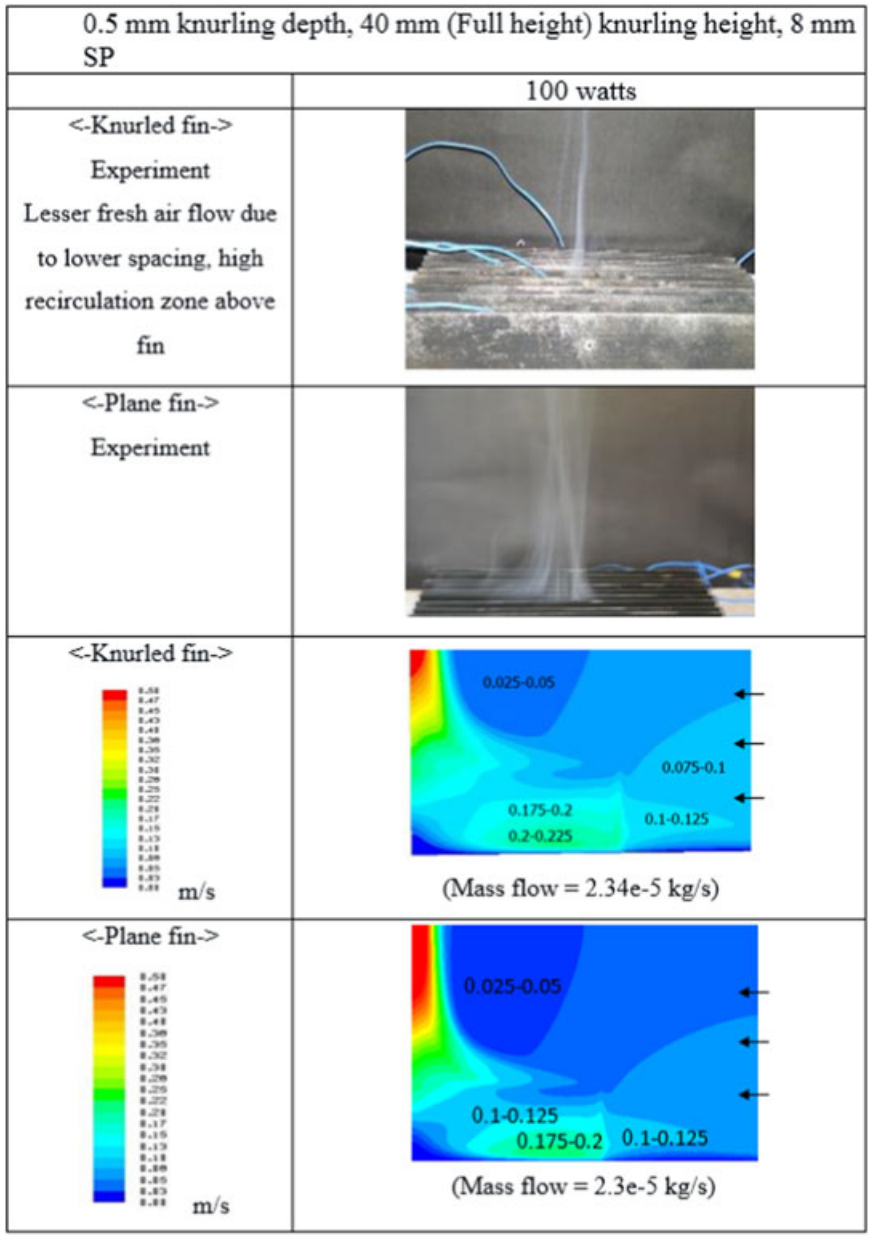

FIGURE 8 Comparison of the experimental and numerical results for knurled and plane fin with 8 mm spacing plane 0.5 mm D_{kn} [Color figure can be viewed at wileyonlinelibrary.com]

7 | COMPARISON OF FLOW PATTERNS—EXPERIMENTAL AND NUMERICAL

Figure 8 shows comparison of flow patterns obtained experimentally[15] for full length of fin and numerically for knurled and plane fins with 8 mm spacing and half-length of fin due to symmetry. The velocity range is plotted from 0 to 0.5 m/s (refer velocity contour plots). Close observation of the flow visualization patterns helps to reveal the differences in flow pattern on

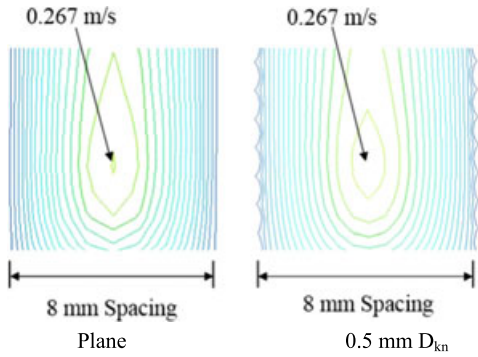

FIGURE 9 Velocity contour plot for knurled and plane fin with 8 mm spacing viewed from side of fin array with plane and 0.5 mm D_{kn} [Color figure can be viewed at wileyonlinelibrary.com]

top of fin array. For 8 mm fin spacing, there exist predominant recirculation zone for both knurled and plane fin; however, the local velocity at knurled fin surface is increased. This is partially attributed to increased mass flow rate from sides of fin array. The velocity range near to fin surface for plane fin is 0.175 to 0.2 m/s, whereas for knurled fin, it is 0.2 to 0.225 m/s. Thus, the average enhancement in flow velocity is around 13%. In Figure 9, the numerical results show that more mass of air is inducted with knurled fin compared with plane fin although interspacing maximum velocity range is almost the same.

Figure 10 compares velocity contours for fins with 0.25 and 0.5 mm roughness depth wherein we see that there is less disturbance of flow in the boundary layer near to the fin wall with lesser roughness depth and thus lesser mass flow.

Figures 11 and 12 show comparison for fin with 10 and 12 mm spacing. The fin roughness depth is 0.5 mm and roughness height is 40 mm. The recirculation zone for knurled fin has reduced to large extent, which eventually helps in drawing more cool air from sides of fin array and thus carrying away more heat.

8 | RESULTS AND DISCUSSION

Table 3 summarizes the major observations for plane, knurled fin with 20 mm and 40 mm roughness height with 0.5 mm roughness depth. Similarly Table 4 summarizes the major observations for 0.25 mm roughness depth with 10 mm spacing at 100 W.

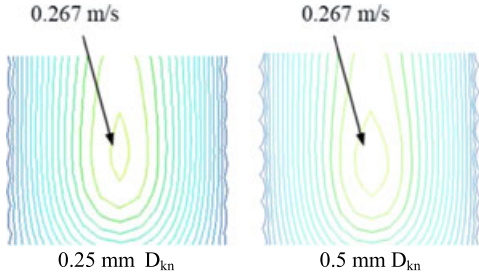

FIGURE 10 Velocity contour plot for knurled fins with 8 mm spacing viewed from side of fin array with 0.25 and 0.5 mm roughness depth [Color figure can be viewed at wileyonlinelibrary.com]

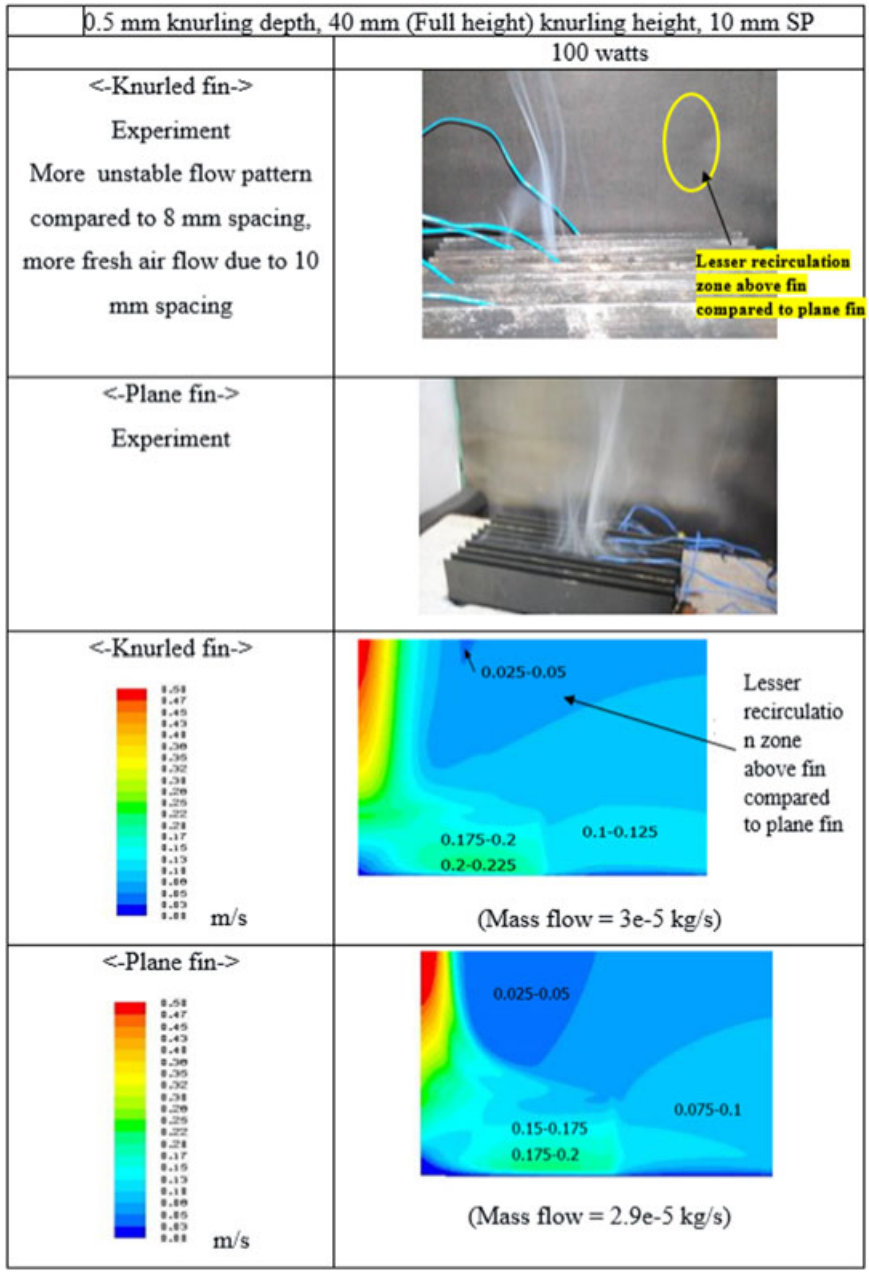

FIGURE 11 Comparison of experimental and numerical results for knurled and plane fin with 10 mm spacing [Color figure can be viewed at wileyonlinelibrary.com]

Figures 13 and 14 show numerical and experimental variation of Nu_a vs Rayleigh number for Plane fin and knurled fin with full knurling height 40 mm, knurling depth 0.25 mm, and different fin spacing. It is clear that for 10 mm spacing, the heat transfer enhancement is higher when compared with 8 and 12 mm spacing. Similarly, Figure 15 and 16 show numerical and experimental variation of Nu_a vs Rayleigh number for knurling depth 0.5 mm and different fin

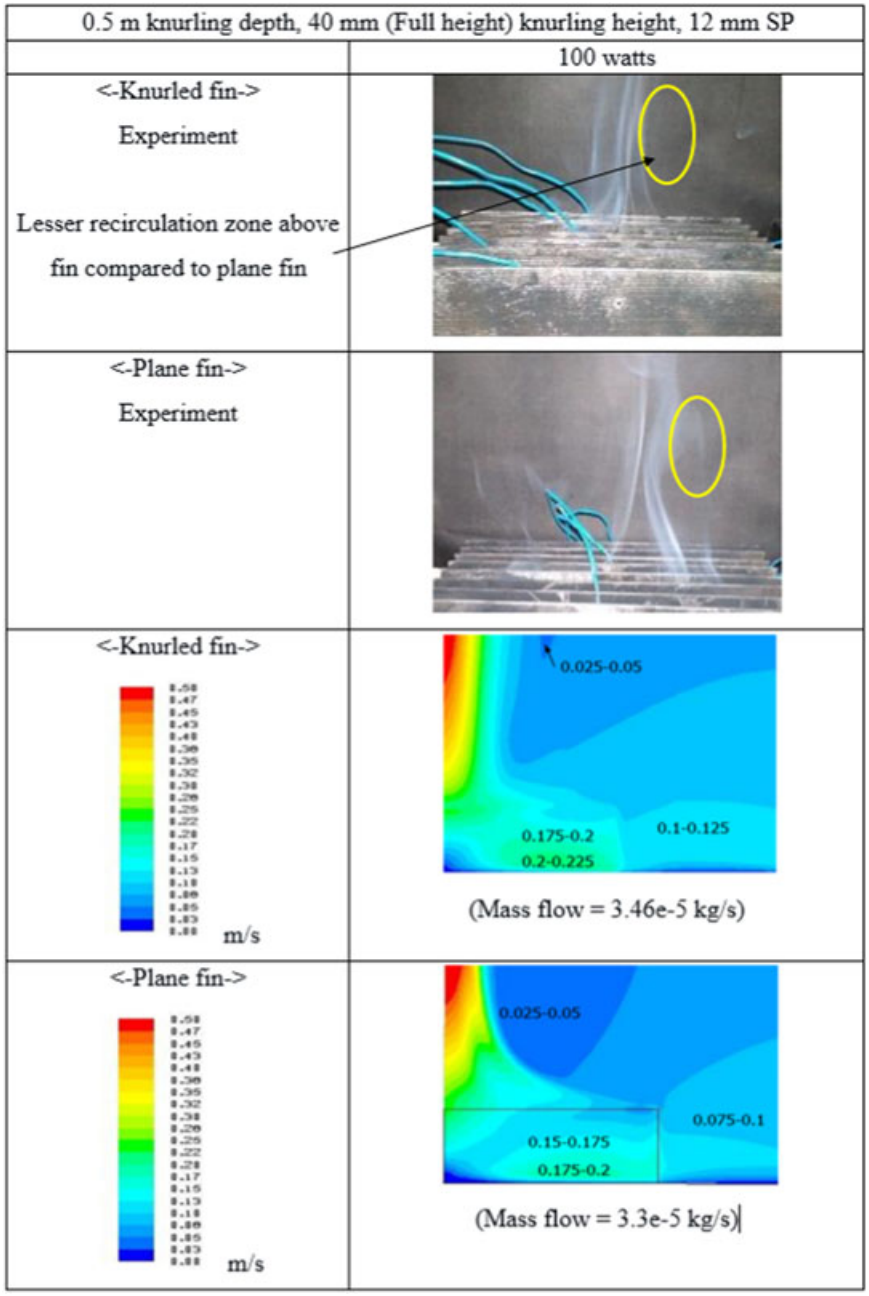

FIGURE 12 Comparison of the experimental and numerical results for knurled and plane fin with 12 mm spacing [Color figure can be viewed at wileyonlinelibrary.com]

spacing. It is also seen that compared with lower roughness depth of 0.25 mm, higher roughness depth gives higher Nusselt number.

Figures 17 and 18 show numerical and experimental variation of Nu_a vs Rayleigh number for plane fin and knurled fin with half knurling height 20 mm, knurling depth 0.25 mm, and different fin spacing. Similarly, Figures 19 and 20 show results for knurling

TABLE 3 Flow behavior comparison for knurled fin with 0.5 mm knurling depth with plane fin

Fin confg→	Comparison aattribute	Plane	0.5 mm D, 20 mm height	0.5 mm D, 40 mm height
SP 8 mm	Recirculation zone Velocity, m/s	High ~0.175 m/s at 100 W	High ~0.2 m/s at 100 W	High ~0.2 m/s at 100 W
SP 10 mm	Recirculation zone Velocity, m/s	High ~0.175 m/s at 100 W	Low ~0.2 m/s at 100 W	Low ~0.2 m/s at 100 W
SP 12 mm	Recirculation zone Velocity, m/s	High ~0.175 m/s at 100 W	High ~0.225 m/s at 100 W	Low ~0.2 m/s at 100 W

TABLE 4 Flow behavior comparison for knurled fin with 0.25 mm knurling depth with plane fin

Fin confg→	Comparison attribute	Plane	0.25 mm D, 20 mm height	0.25 mm D, 40 mm height
SP 10 mm	Recirculation zone Velocity, m/s	High ~0.175 m/s at 100 W	Slightly lower ~0.175 m/s at 100 W	Slightly lower ~0.2 m/s at 100 W

depth 0.5 mm and different fin spacing. Similar explanation of physical reasoning can be given as that for full knurling height and Section 7 above. Further Figure 21A and B compares the experimental and numerical results for knurled fin with full roughness height 40 mm and roughness depth 0.25 mm and 0.5 mm respectively. It is observed that results from numerical simulation follows the same trend as experiments; however, deviation at 8 mm spacing may be attributed to the K-ω SST turbulence model unable to capture flow physics at lower fin spacing. Another reason might be due to the difference

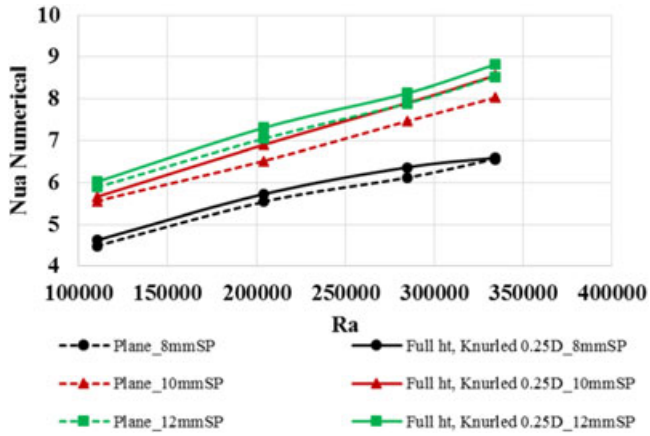

FIGURE 13 Variation of Nu_a numerical vs Rayleigh number for different fin spacing, plane fin, and knurled fin with full knurling height 40 mm and knurling depth 0.25 mm [Color figure can be viewed at wileyonlinelibrary.com]

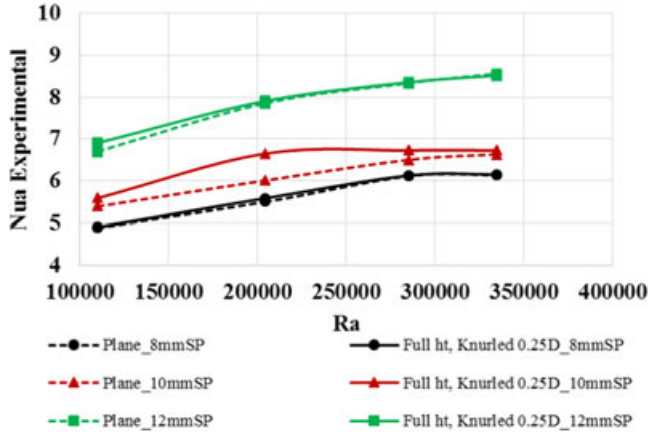

FIGURE 14 Variation of Nu_a experimental vs Rayleigh number for different fin spacing, Plane fin, and knurled fin with full knurling height 40 mm and knurling depth 0.25 mm [Color figure can be viewed at wileyonlinelibrary.com]

between actual knurling on fins by manufacturing and mesh profile generated in preprocessing for numerical analysis.

Figure 22A and 22B compares experimental and numerical results for knurled fin with half roughness height 20 mm and roughness depth 0.25 mm and 0.5 mm, respectively and for all fin spacing considered. It is observed that % enhancement in Nu_a is over predicted in numerical analysis.

8.1 | Effect of nondimensional parameters on Nusselt number

8.1.1 | Effect of variation in S/H on Nu

Figure 23A and 23B show effect of parameter S/H on Nusselt number. By increasing this parameter, the side area of fin array increases, which inducts more amount of mass of air

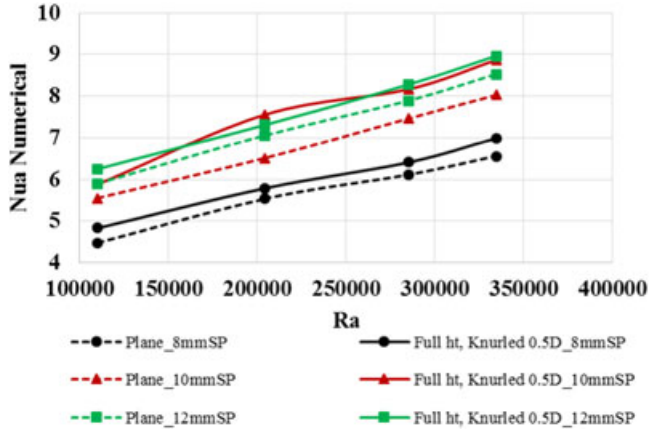

FIGURE 15 Variation of Nu_a numerical vs Rayleigh number for different fin spacing, plane fin, and knurled fin with full knurling height 40 mm and knurling depth 0.5 mm [Color figure can be viewed at wileyonlinelibrary.com]

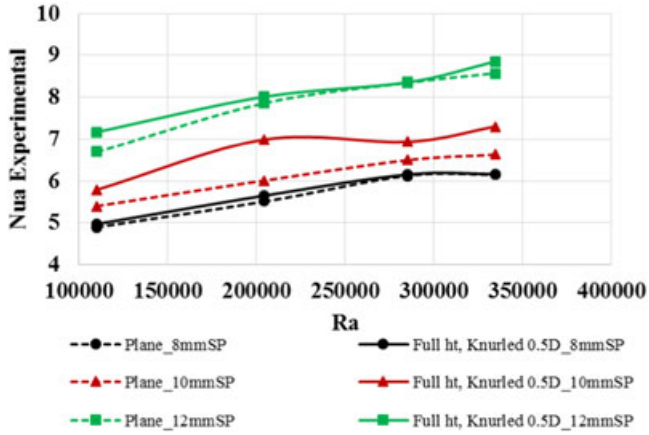

FIGURE 16 Variation of Nu_a experimental vs Rayleigh number for different fin spacing, plane fin, and knurled fin with full knurling height 40 mm and knurling depth 0.5 mm [Color figure can be viewed at wileyonlinelibrary.com]

thereby increasing the heat transfer rate. Other parameters like Rayleigh number, knurling height, and depth are kept constant. Variation of Nusselt number beyond this range can be found by further experimentation; however, it is beyond the scope of the present work.

8.1.2 | Effect of variation in H_{kn}/H on Nu

Figure 24A and 24B show effect of fin roughness parameter H_{kn}/H on Nusselt number. With knurling depth and Rayleigh number held constant, the knurling height has marginal effect on the heat transfer rate. The value of $H_{kn}/H = 0$ corresponds to plane fin, 0.5 for half height fin, and 1 for full height fin. We see that knurling on fins increase the heat transfer rate when compared with the plane fin.

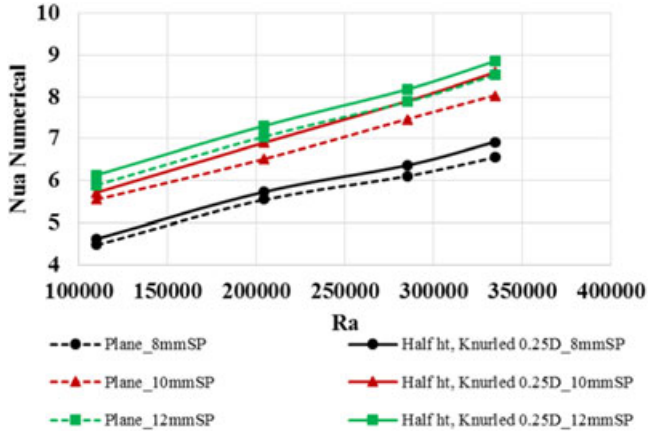

FIGURE 17 Variation of Nu_a numerical vs Rayleigh number for different fin spacing, plane fin, and knurled fin with half knurling height 20 mm and knurling depth 0.25 mm [Color figure can be viewed at wileyonlinelibrary.com]

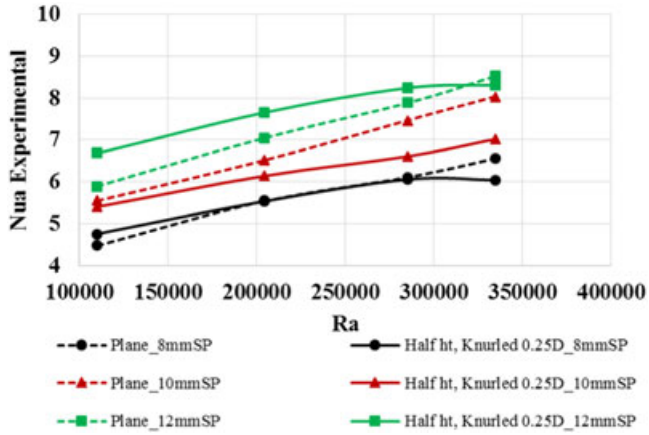

FIGURE 18 Variation of Nu_a experimental vs Rayleigh number for different fin spacing, plane fin, and knurled fin with half knurling height 20 mm and knurling depth 0.25 mm [Color figure can be viewed at wileyonlinelibrary.com]

8.1.3 | Effect of variation in D_{kn}/H on Nu

Similarly Figure 25A and 25B show effect of fin roughness parameter D_{kn}/H on Nusselt number. With knurling height and Rayleigh number held constant, the knurling depth has strong effect on heat transfer rate. The value of $D_{kn}/H = 0$ corresponds to plane fin, 0.006 for 0.25 mm depth and 0.13 for 0.5 mm depth across fin thickness.

For fin with half knurling height, the depth effect is seen to be higher compared with full knurling height. More the roughness depth, more disturbance to the flow in laminar sublayer giving rise to unstable flow near wall and thus increased velocity causes augmentation of heat transfer. It is observed that the heat transfer rate for fin with 0.5 mm depth increases two-folds when compared with the fin with 0.25 mm depth.

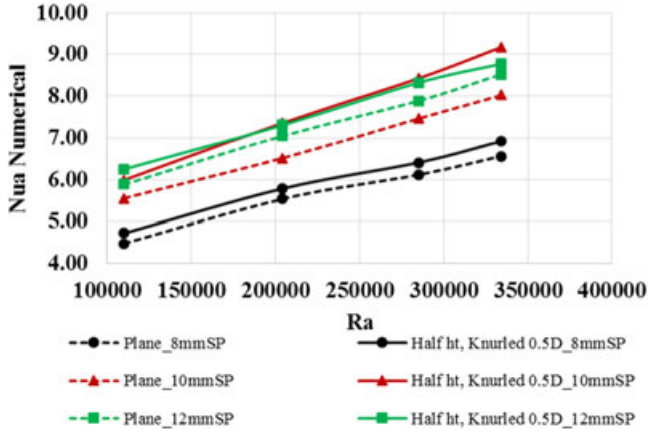

FIGURE 19 Variation of Nu_a numerical vs Rayleigh number for different fin spacing, plane fin, and knurled fin with half knurling height 20 mm and knurling depth 0.5 mm [Color figure can be viewed at wileyonlinelibrary.com]

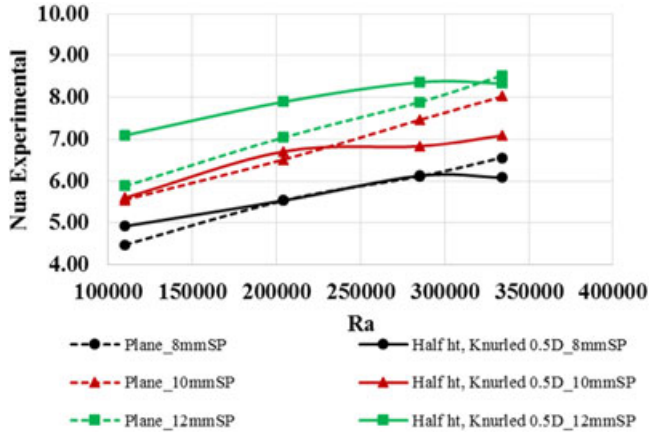

FIGURE 20 Variation of Nu_a experimental vs Rayleigh number for different fin spacing, plane fin, and knurled fin with half knurling height 20 mm and knurling depth 0.5 mm [Color figure can be viewed at wileyonlinelibrary.com]

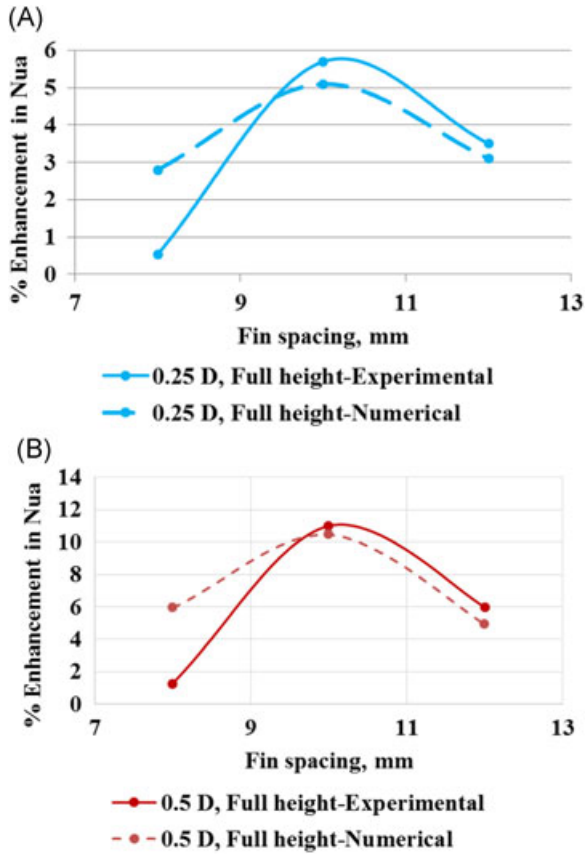

FIGURE 21 A, Comparison of experimental and numerical results for full knurling height 40 mm and knurling depth 0.25 mm. B, Comparison of experimental and numerical results for full knurling height 40 mm and knurling depth 0.5 mm [Color figure can be viewed at wileyonlinelibrary.com]

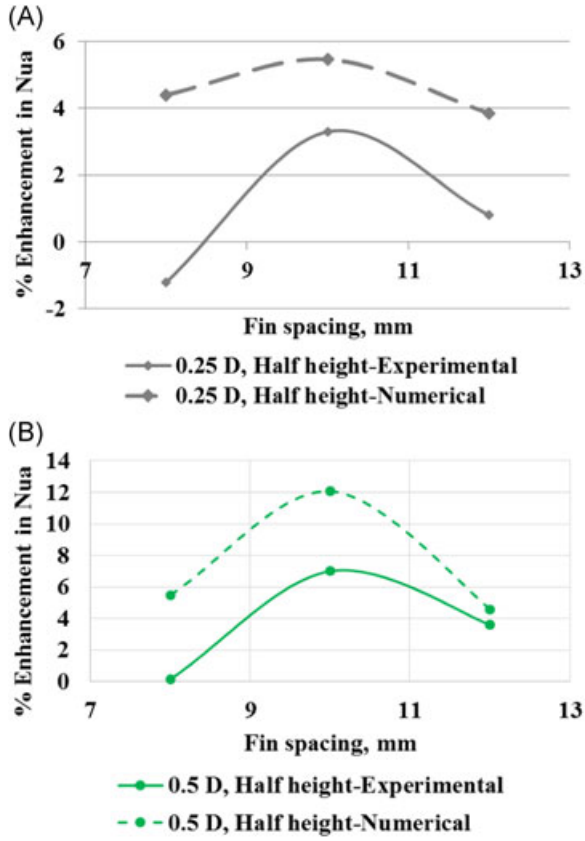

FIGURE 22 A, Comparison of experimental and numerical results for half knurling height 20 mm and knurling depth 0.25 mm. B, Comparison of experimental and numerical results half knurling height 20 mm and knurling depth 0.50 mm [Color figure can be viewed at wileyonlinelibrary.com]

9 | CORRELATION FOR NUSSELT NUMBER

The functional relationship between Nusselt number Nu_a and independent parameter groupings in dimensionless form can be written as

$$Nu_a = Nu_a\left(Ra, \frac{S}{H}, \frac{D_{kn}}{H}, \frac{H_{kn}}{H}\right). \tag{8}$$

Following independent parameter groupings in dimensionless form are identified using Buckingham pi theorem, Ra is the Rayleigh number, S/H is the spacing to fin height ratio, D_{kn}/H is the knurling depth to fin height ratio, and H_{kn}/H is the knurling height to fin height ratio.

Nu_a vs Ra is plotted with available data points from numerical simulation as shown in Figure 26. On the basis of nonlinear regression analysis of the available data points,[16] the following correlation is obtained using POLYMATH 6.10

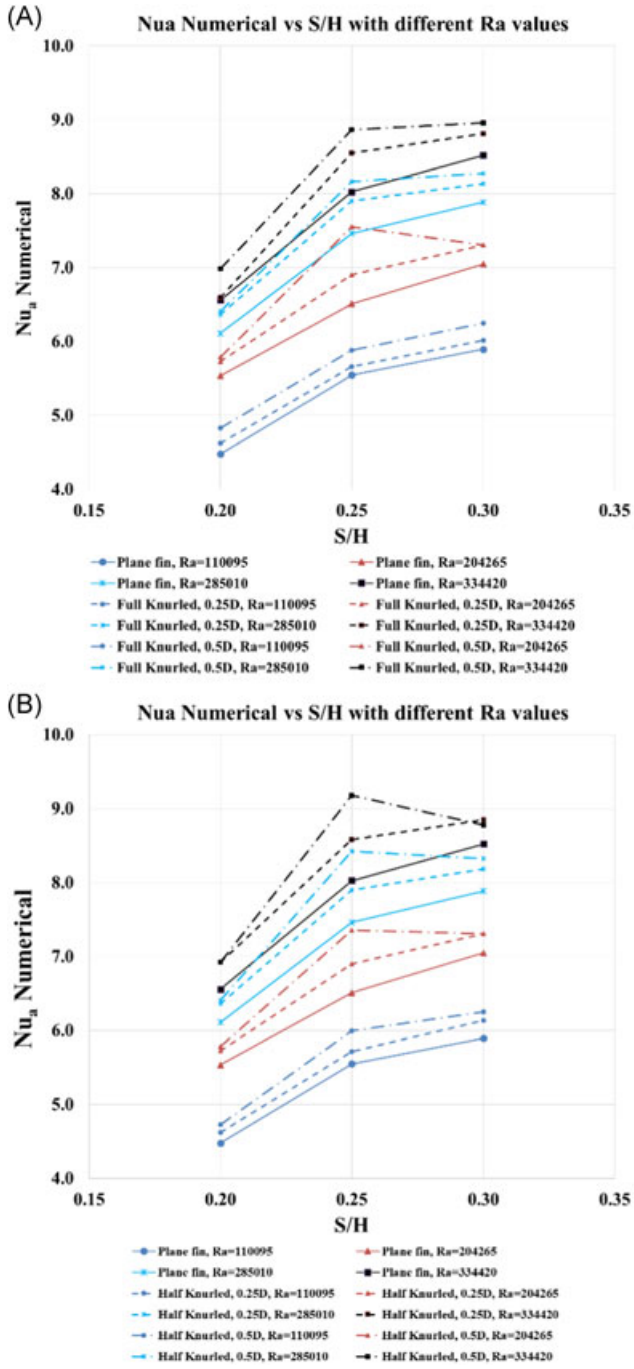

FIGURE 23 A, Effect of parameter S/H on Nusselt number for full knurled fin. B, Effect of parameter S/H on Nusselt number for half knurled fin [Color figure can be viewed at wileyonlinelibrary.com]

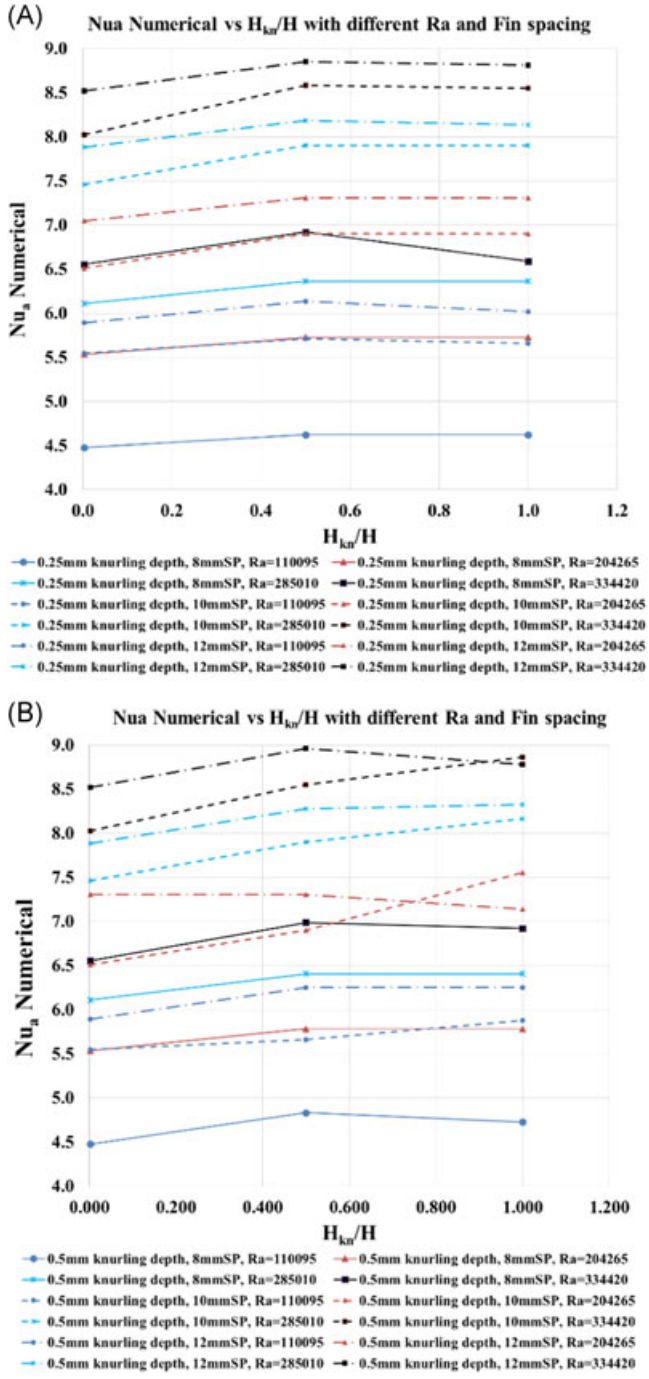

FIGURE 24 A, Effect of parameter H_{kn}/H on Nusselt number for 0.25 mm knurling depth. B, Effect of parameter H_{kn}/H on Nusselt number for 0.5 mm knurling depth [Color figure can be viewed at wileyonlinelibrary.com]

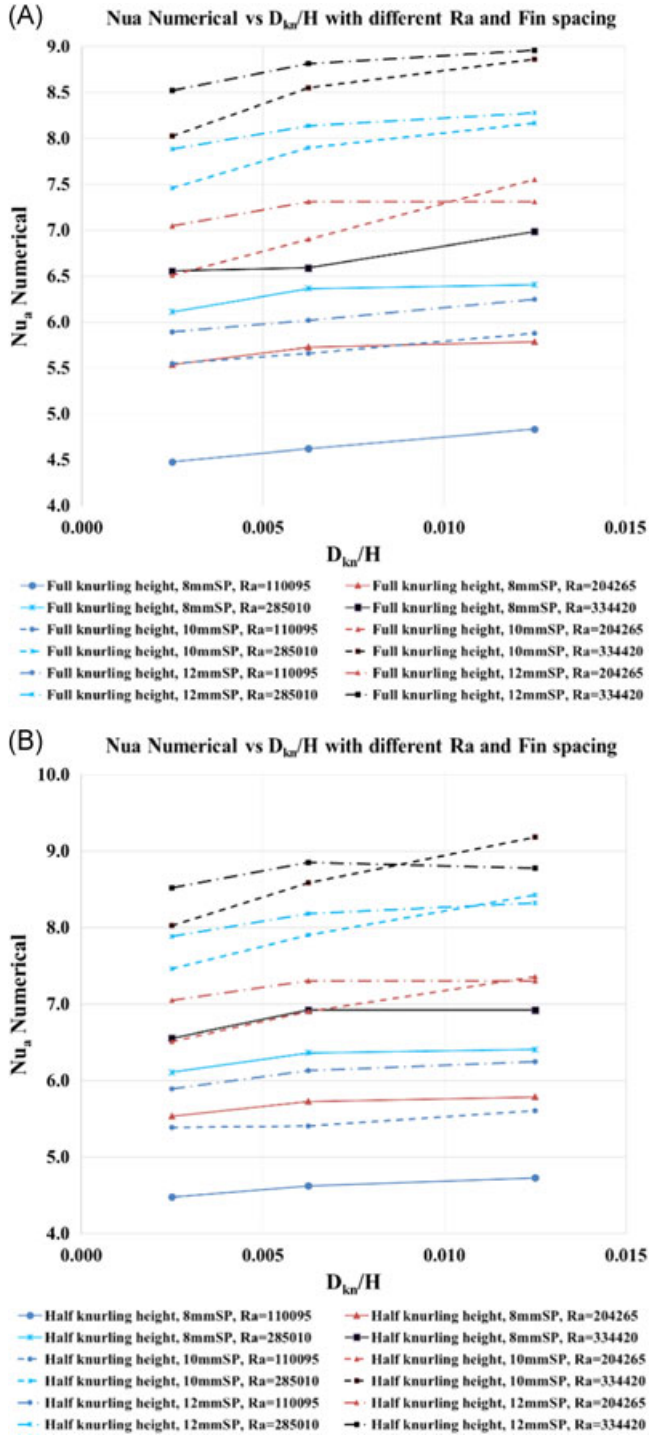

FIGURE 25 A, Effect of parameter D_{kn}/H on Nusselt number for full knurled fin. B, Effect of parameter D_{kn}/H on Nusselt number for half knurled fin [Color figure can be viewed at wileyonlinelibrary.com]

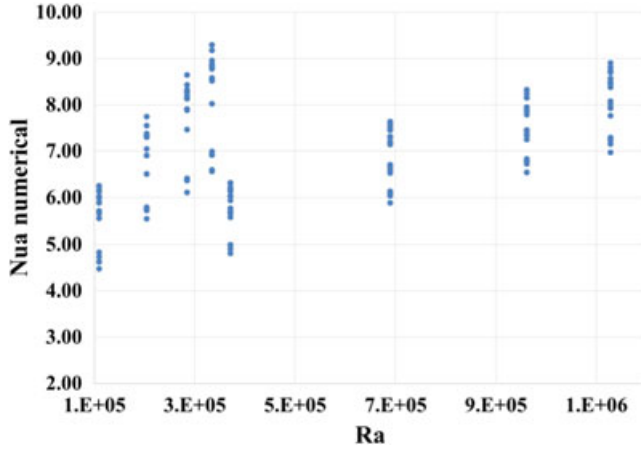

FIGURE 26 Nu_a vs Ra for all knurl fin configurations [Color figure can be viewed at wileyonlinelibrary.com]

$$Nu_a = 1.302Ra^{0.2092}\left(\frac{S}{H}\right)^{0.5726}\left(\frac{D_{kn}}{H}\right)^{0.0251}\left(\frac{H_{kn}}{H}\right)^{0.0064}. \quad (9)$$

The above Equation (9) is valid in below limits

$1 \times 10^5 < Ra < 1.2 \times 10^6$

$0.2 < S/H < 0.35$

$0 < D_{kn}/H < 0.013$

$0 < H_{kn}/H < 1$

Pr~0.7

For Equation (9), the coefficient of determination (R^2) is 0.82 and variance is 0.24. Above correlation equation is derived based on the available numerical data points; however, this form of the equation is suitable for predicting heat transfer from knurled fins in terms of fin roughness parameters. Figure 27 shows comparison of predicted Nusselt number using above correlation and numerical Nusselt numbers.

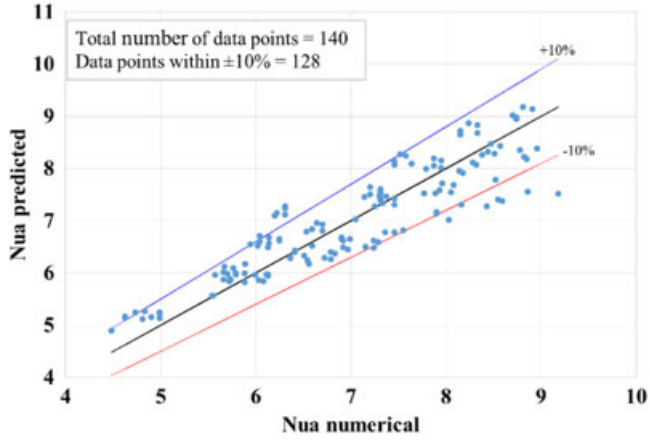

FIGURE 27 Nu_a predicted vs Nu_a numerical for knurl fin configuration [Color figure can be viewed at wileyonlinelibrary.com]

10 | CONCLUSIONS

Numerical study of Natural convection heat transfer is carried out for horizontal base vertical fin array consisting of plane fins and knurled fins with various knurling height and depth configurations. Numerical model is checked for grid independency and also validated against experimental data from the literature. Flow characteristics from numerical and experiments for plane and knurled fin configurations are compared. More attention is devoted to understand flow physics and heat transfer phenomena and effect of knurling on flow is studied. The results are plotted in terms of average Nu_a vs Ra for various fin spacing and values compared with experimental data. Also the effect of nondimensional roughness parameters are assessed for effect on Nusselt number. Further, a correlation for Nusselt number in terms of Rayleigh number and fin roughness parameters is proposed.

Following conclusions are drawn from the above study

(1) Knurled fin with full knurling height of 40 mm, knurl depth of 0.5 mm, and spacing between fin 10 mm gives maximum augmentation of Nusselt number by 15%. Thus, knurled fins may be used for practical purposes where space or cost limit incorporation of other means of augmentation.

(2) Reduction in recirculation zone above knurled fin array compared to that in plane fin is clearly seen in numerical simulation. Also there is an increase in velocity range near to knurled fin surfaces by around 5% to 15% when compared with the plane fin.

(3) It is further observed that percentage of enhancement in Nusselt number obtained from numerical simulation agrees well with that from experiments of full height knurl fin configurations; however, deviation is observed for half height knurl fin configurations. This may be attributed to numerical error, the turbulence model not able to capture flow physics exactly consisting of high instabilities during experiments. This necessitates further optimizing turbulence model constants.

(4) Nondimensional roughness depth and spacing (D_{kn}/H and S/H) have more effect on Nusselt number than roughness height (H_{kn}/H). This is due to the fact that flow quantities near the wall get affected in presence of knurling on fins whether it is full knurled or half knurled fins.

(5) Finally, the proposed correlation agrees well with the numerical results within 10% accuracy. The proposed correlation can be used to assess knurled fin performance and reduce the cost of experimentation.

NOMENCLATURE

D_{kn}	Knurling (or roughness) depth (mm)
Gr_L	Grashof number based on characteristic length L
g	Gravitational constant (9.81 m/s^2)
H_{kn}	Knurling (or roughness) height (mm)
H	Fin height (mm)
h_{avg}	Average heat transfer coefficient (W/m^2·K)
k	Thermal conductivity of fluid (W/m·K)
L	Characteristic length (mm)
Nu_L	Nusselt number based on characteristic length L

Nu_a Average Nusselt number
Pr Prandtl number
Ra_L Rayleigh number based on characteristic length L
S Fin spacing (mm)
Ts Average fin surface temperature (K)
T_∞ Ambient temperature (K)
u, v, w Velocity components in x, y, and z directions (m/s)

NONDIMENSIONAL PARAMETERS

S/H Nondimensional fin spacing
D_{kn}/H Nondimensional roughness depth
H_{kn}/H Nondimensional roughness height

GREEK SYMBOLS

ρ Fluid density, kg/m^3
ρ_a Reference density, kg/m^3
α Thermal diffusivity (m^2/s)
β Thermal expansion coefficient (1/K)
υ Kinematic viscosity (m^2/s)
Δ Change in variable

SUBSCRIPTS

kn Knurling
avg Average

CONFLICT OF INTERESTS

The authors declare that there are no conflict of interests.

ORCID

Rahul C. Chikurde http://orcid.org/0000-0003-4392-656X

REFERENCES

1. Baskaya S, Sivrioglu M, Ozek M. Parametric study of natural convection heat transfer from horizontal rectangular fin arrays. *Int J Therm Sci*. 2000;39:797-805.
2. Bhavnani SH, Bergles AE. Effect of surface geometry and orientation on laminar natural convection heat transfer from a vertical flat plate with transverse roughness elements. *Int J Heat Mass Trans*. 1990;33(5):965-981.
3. Kwak CE, Song TH. Experimental and numerical study on natural convection from vertical plates with horizontal rectangular grooves. *Int J Heat Mass Trans*. 1998;41(16):2517-2528.
4. Jiang L. Experimental and numerical investigation of convection heat transfer in a rectangular channel with angled ribs. *Exp Therm Fluid Sci*. 2006;30:513-521.
5. Chaube A, Sahoo PK, Solanki SC. Analysis of heat transfer augmentation and flow characteristics due to rib roughness over absorber plate of a solar air heater. *Renew Energy*. 2006;31:317-331.

6. Layek A, Saini JS, Solanki SC. Heat transfer and friction characteristics for artificially roughened ducts with compound turbulators. *Int J Heat Mass Trans*. 2007;50:4845-4854.
7. Ashjaee M, Amiri M, Rostami J. A correlation for free convection heat transfer from vertical wavy surfaces. *Heat Mass Trans*. 2007;44:101-111.
8. Shaeri MR, Yaghoubi M. Numerical analysis of turbulent convection heat transfer from an array of perforated fins. *Int J Heat Fluid Flow*. 2009;30:218-228.
9. Ismail MF, Reza MO, Zobaer MA, Ali M. Numerical investigation of turbulent heat convection from solid and longitudinally perforated rectangular fins. *Procedia Eng*. 2013;56:497-502.
10. Ismail F, Hasan M, Saha SC. Numerical study of turbulent fluid flow and heat transfer in lateral perforated extended surfaces. *Energy*. 2014;64:632-639.
11. Shadlaghani A, Tavakoli MR, Farzaneh M, Salimpour MR. Optimization of triangular fins with/without longitudinal perforate for thermal performance enhancement. *J Mech Sci Technol*. 2016;30(4):1903-1910.
12. Raut SV, Kothavale BS, Chikurde RC. Experimental study of natural convection heat transfer with horizontal rectangular fin array using various knurling patterns on fin. *Int Eng Res J*. 2017:1-7. Special Edition PGCON-MECH-2017. http://www.ierjournal.org/pgcon2017.php
13. Chikurde RC, Kothavale BS, Sane NK, Dingare SV. Convection heat transfer studies on rectangular fin arrays with different surface roughness, perforations or protrusions on fins—a review. *Int Rev Mech Eng (IREME)*. 2018;12(1):97-106. *Special section on "ICMESCoE-2017."*
14. Harahap F, McManus N. Natural convection heat transfer from horizontal rectangular fin arrays. *ASME J Heat Trans*. 1967;89(1):32-38.
15. Chikurde RC, Kothavale BS, Sane NK. *Natural convection heat transfer with horizontal rectangular fin array using straight knurling patterns on fins—an experimental study*. ASME International Mechanical Engineering Congress and Exposition (IMECE) Pittsburgh, USA; 2018. doi: https://doi.org/10.1115/IMECE2018-86449
16. Senapati JR, Dash SK, Roy S. Numerical investigation of natural convection heat transfer over annular finned horizontal cylinder. *Int J Heat Mass Transfer*. 2016;96:330-345.

How to cite this article: Chikurde RC, Kothavale BS, Sane NK. Numerical validation of natural convection heat transfer with horizontal rectangular fin array using straight knurling patterns on fins—correlation for Nusselt number. *Heat Transfer—Asian Res*. 2019;1-26. https://doi.org/10.1002/htj.21449